Meccanica (2007) 42:423–433
DOI 10.1007/s11012-007-9066-6

Cycle-to-cycle oscillations of heat release in a spark ignition engine

Grzegorz Litak · Tomasz Kamiński · Jacek Czarnigowski · Dariusz Żukowski · Mirosław Wendeker

Received: 12 November 2005 / Accepted: 12 March 2007 / Published online: 2 June 2007

Abstract Fluctuations of combustion were studied using experimental time series of internal pressure in one of four cylinders in a spark ignition engine. Employing standard statistical methods like histograms and return maps, cycle-to-cycle variations of heat release were analyzed. A substantial difference in system behavior corresponding to quality of combustion was observed with a changing spark advance angle. Examining recurrence plots for a higher spark advance angle formation of specific patterns of vertical lines characteristic to intermittent behavior was found.

G. Litak (✉) · D. Żukowski
Department of Applied Mechanics, Technical University of Lublin, Nadbystrzycka 36, 20-618, Lublin, Poland
e-mail: g.litak@pollub.pl

G. Litak
Institut für Mechanik und Mechatronik, Technische Universität Wien, Wiedner Hauptstraße 8-10, Wien 1040, Austria

T. Kamiński
Motor Transport Institute, ul. Jagiellońska 80, Warsaw 03-301, Poland

J. Czarnigowski
Department of Machine Construction, Technical University of Lublin, Nadbystrzycka 36, 20-618, Lublin, Poland

M. Wendeker
Department of Combustion Engines, Technical University of Lublin, Nadbystrzycka 36, 20-618, Lublin, Poland

Keywords Spark ignition engine · Combustion · Time series analysis · Recurrence plot · Mechanics of machines

1 Introduction

Instabilities of combustion, observed long ago [1], appeared to be a permanent feature of any combustion engine [2]. Unfortunately these obstacles remain present in modern engines and they cause many problems in engine control [3–8]. Identification of their sources and consideration of methods for their elimination have emerged among the main issues in spark ignition engine technologies engineering in the last century [9–15]. Their sources were initially classified by Heywood [10] as aerodynamics in the cylinder during combustion and variation in the amounts of fuel, air, and recycled exhaust gas supplied to the cylinder and a local mixture composition near the spark plug. These concepts were explored originally by Winsor and Patterson [16], Hu [11] who invoked a turbulent combustion process, and Daily [17] who studied an exhaust gas recycling process. On the other hand, Foakes and Pollard [18], Chew et al. [19], and Letellier et al. [20] used a systematical approach of nonlinear methods to analyze pressure time series and even performed ingenious Lyapunov exponents calculations [20]. A breakthrough in understanding the origin of combustion instabilities was given by Daw et al. [21,22] and later by Rocha-Martinez et al. [23], Litak et al. [24], who invented

simplified models of exhaust gas recirculation drawing attention to non-periodic heat release time series. The strongest evidences for nonlinear dynamics in combustion came from statistical properties of experimental signals time irreversibility of related heat release time series, as has been shown by Green et al. [25], Wagner et al. [12]. An interesting application of symbolic analysis to cyclic heat release time series has been discussed in detail by Daw et al. [13]. On the other hand, Wendeker et al. [26] exploring pressure time series found intermittency mechanism leading to chaotic combustion. Recently Sen et al. [27] has applied the wavelet analysis to pressure time series and found short harmonics in the wavelet power spectra which gave a further evidence of intermittent behaviors in pressure fluctuations. In the present paper, the statistical properties of heat release time series are examined. After the present introduction (Sect. 1), a description of the experimental facilities and discussion of the procedure used for performing measurements is given in Sect. 2. In this section examples of cycle-to-cycle variations in pressure inside one of the cylinders are also shown. In the next section (Sect. 3), the statistical properties of heat release time series are examined. To this end in Sect. 4 the summary and concluding remarks are presented.

2 Experimental facilities and measurements

Experimental results presented in this paper were obtained using a piezo-electric sensor applied to measure pressure inside an engine cylinder. It should be noted that pressure is the best known quantity directly measured to analyze engine dynamics [4,5,10,28–30]. Actual cylinder pressure together with present internal cylinder volume can be used to obtain indicated mean effective pressure (IMEP), to calculate some useful quantities as: the engine torque and indicated efficiency, and also to estimate important combustion quantities as burn rate, bulk temperature, and heat release [10]. Moreover, statistical analysis of the internal pressure data can also provide information about combustion process stability. The equipment used in this study provides one of the direct measures of combustion quality in an internal combustion engine.

The present internal pressure data were obtained from the Engine Laboratory of Technical University of Lublin, where a series of tests was conducted. The pressure traces were obtained on a 1,998 cm^3 Holden 2.0 MPFI engine at 1,000 rpm. Measurements were conducted with a resolution of about 0.7° of crankshaft revolution. Each experimental test contained about 2,000 cycles of engine work. Data was taken at different spark timings (spark advance angles): 5, 15, 30 degrees before top dead center (TDC). The engine speed, air/fuel ratio, and throttle setting were all held constant throughout the data collection period. Intake manifold pressure was 40 kPa. A stoichiometric mixture ($\lambda \approx 1$) was used in these experiments.

Figure 1 illustrates results of pressure data, purposely limited to the first five cycles of the combustion process for three values of spark advance angles $\Delta\alpha = 5°, 15°, 30°$. The change in pressure oscillations, which is often described in terms of cyclic pressure maxima $p_{\max}$ variations [30], can be noticed, as well as the corresponding angles α_{pmax}. The obtained oscillations have been measured in after in phase of engine stable work and they were not associated with drift terms during warm-up phase. In the next section cyclic heat release analysis for all three cases is presented.

3 Analysis of heat release

To capture the cycle-to-cycle changes in the combustion process heat release Q_i was calculated for a sequence of about 2,000 consecutive combustion cycles. This quantity is more convenient for analysis than pressure itself because the periodic pressure oscillations due to compression and expansion strokes are integrated out. Heat release also has practical meaning as it is proportional to burned fuel mass [10].

During the combustion process the internal volume of engine cylinder is driven kinematically by the piston. As a consequence of this, the volume also changes periodically as a function of a crank angle α and satisfies the relation:

$$V(\alpha) = \pi \frac{D^2}{4} h + \pi \frac{D^2}{4} 2r \frac{1}{\varepsilon - 1}, \tag{1}$$

where the piston position, h, is given by

$$h = r(1 - \cos\alpha) + l_0 \left(1 - \frac{r}{l} \sqrt{\frac{l^2}{r^2} - \sin^2\alpha} \right), \tag{2}$$

and geometrical constants r, l_0, D as well as ε are defined in Table 1.

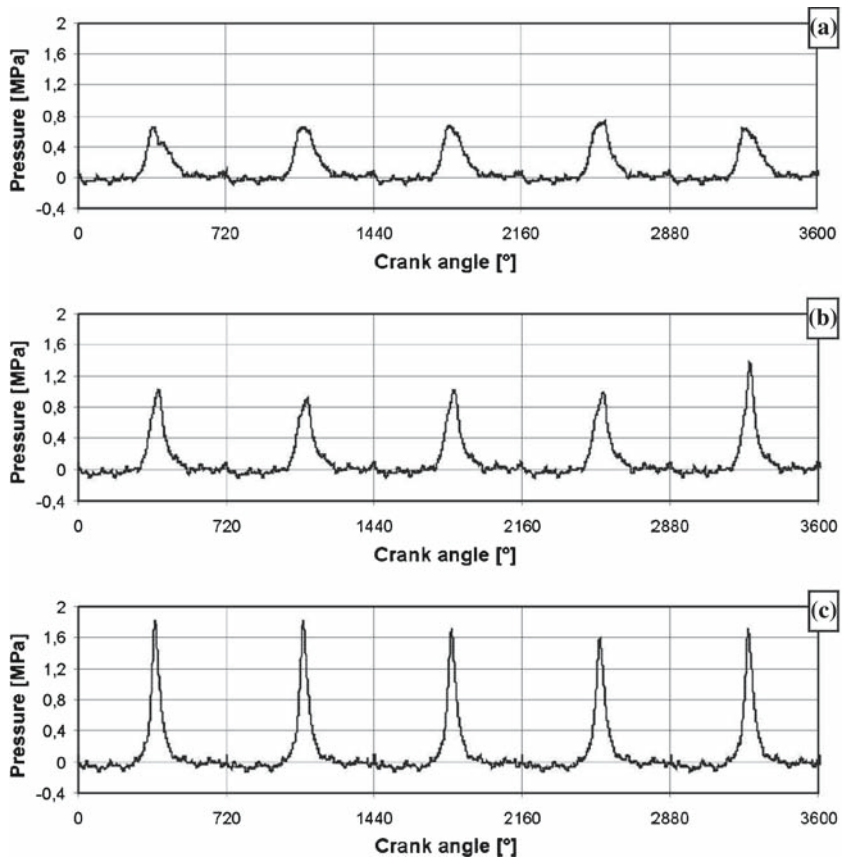

Fig. 1 Pressure time series of first five consecutive cycles measured inside one of four cylinders for different spark advance angles. (**a**) $\Delta\alpha = 5°$,(**b**) $\Delta\alpha = 15°$, (**c**) $\Delta\alpha = 30°$

For an adiabatic process heat released in chemical reactions during combustion in the engine cylinder is given by an differential equation coming from the first law of thermodynamics with respect to the angle α:

$$\frac{\mathrm{d}Q}{\mathrm{d}\alpha} = \frac{\kappa}{\kappa - 1} p \frac{\mathrm{d}V}{\mathrm{d}\alpha} + \frac{1}{\kappa - 1} V \frac{\mathrm{d}p}{\mathrm{d}\alpha}. \tag{3}$$

Using it together with the pressure time series and parametric change of cylinder volume V Eqs. 1–2 we have performed calculations of heat released in consecutive cycles Q_i [15], closely related to burned fuel mass M_i per cycle:

$$M_i \approx Q_i / W_u, \tag{4}$$

where W_u is a heating value of the fuel, listed in Table 1. It should be underlined that the last equation (Eq. 4) neglects the effects of heat transfer between the cylinder chamber and its walls in spirit of an adiabatic process (Eq. 3). For non-stoichiometric combustion, the consumed mass M_i should be slightly larger because it also depends on the quality of mixture and the combustion process.

3.1 Cycle-to-cycle fluctuations of heat release

In Fig. 2 the calculated heat release Q_i, for $N = 1,991$ cycles is plotted against cycles i for $\Delta\alpha = 5, 15, 30$ degrees, respectively. Because in all cases Q_i changes between some finite values it is obvious that there are no misfires in the heat release data, presented here [31].

Note the average values of heat release $\langle Q_i \rangle$ are comparable in all cases $\langle Q_i \rangle = 352\,\mathrm{J}$ (for $\Delta\alpha = 5°$) $\langle Q_i \rangle = 394\,\mathrm{J}$ (for $\Delta\alpha = 15°$) $\langle Q_i \rangle = 375\,\mathrm{J}$ (for $\Delta\alpha = 30°$). $\langle Q_i \rangle$ is the smallest for $\Delta\alpha = 5°$ indicating the lowest burning rate of fuel for this case. The corresponding standard deviations are $\sigma_Q = 33\,\mathrm{J}$, $\sigma_Q = 25\,\mathrm{J}$, $\sigma_Q = 26\,\mathrm{J}$. On the other hand, the output torque, for the same rotational velocity of the crankshaft,

Table 1 Definitions of variables and symbols used in the paper

Position of the piston	h
Internal cylinder pressure	P
Actual cylinder volume	$V(\alpha)$
Heat release	Q
Heat released in particular cycle i	Q_i or $Q(i)$
Average value of heat release	$\langle Q_i \rangle$
Standard deviation of heat release variations	σ_Q
Spark advance angle	$\Delta\alpha$
Cycle number	i, j
Number of considered points in time series	N
Threshold value	ϵ
Loading torque	F
Crank angle	$\alpha \in [0, 720°]$
Cylinder diameter	$D = 86\,\text{mm}$
Crank radius	$r = 43\,\text{mm}$
Connecting-rod length	$l_0 = 143\,\text{mm}$
Heating value of the fuel	$W_u = 43000\,\text{kJ/kg}$
Compression ratio	$\varepsilon = 8.8$
poisson constant	$\kappa = \frac{c_p}{c_v} \approx 1.4$
Mass burned in cycle i	M_i
Excess-air factor	λ
Recurrence rate	RR
Determinism	DET
Trapping time	TT
Laminarity	LAM
Maximal diagonal length	$L_{\max}$
Maximal vertical length	$V_{\max}$
Entropy of diagonal lines	L_{ENTR}
Entropy of vertical lines	V_{ENTR}
Heaviside function	$\Theta(x)$
Recurrence plot matrix	$\mathbf{R}^{m,\epsilon}$
Recurrence plot matrix elements	$R_{ij}^{m,\epsilon}$
Heat release in the embedding space	$\mathbf{Q}_i$
Length and minimal length of diagonal (vertical) lines	$l, l_{\min} = 2\,(v, v_{\min} = 2)$
Probability of diagonal (and vertical) linens of given length	$p(l),\ l\,(p(v),\ v)$

was relatively large $F = 30\,\text{Nm}$ in the case $\Delta\alpha = 30°$ comparing to other levels $F = 21$ and $28\,\text{Nm}$ for $\Delta\alpha = 5°$ and 15°, respectively.

To be more precise in analysis of fluctuations around $\langle Q_i \rangle$ corresponding histograms were plotted

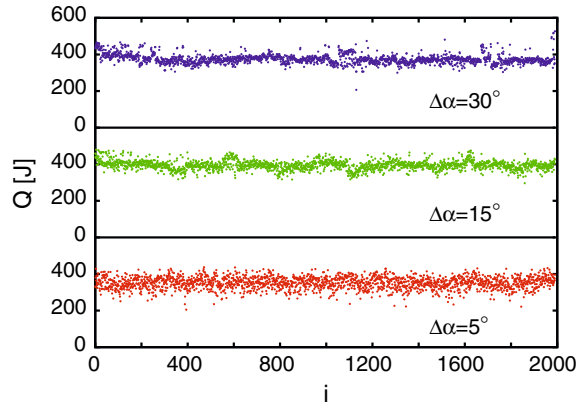

Fig. 2 Heat release Q in consecutive cycles for different spark advance angles: $\Delta\alpha = 5°$, $\Delta\alpha = 15°$, $\Delta\alpha = 30°$

(Fig. 3a–c), as were return maps (Fig. 4a–c). Histograms give information about the distribution of Q_i points. Note that for $\Delta\alpha = 5°$ and 15° (Fig. 3a, b) the distribution is nearly Gaussian. In this case it can also be observed that the standard deviation σ_Q decreases for a larger spark advance angle $\Delta\alpha$. Note, for $\Delta\alpha = 30°$ (Fig. 3c) a substantially different kind of distribution is observed. The long tail, on the right hand side, can be a precursor of an exponential distribution, frequently observed in some sudden change in system behavior such as a surface damage in technological processes [32] or other dynamical systems with intermittent motion. It could be also associated with creation of the second peak of probability with higher heat release. Such explanation can be also motivated by Fig. 2 (upper panel $\Delta\alpha = 30°$) where some combustion events are observed to have relatively high heat release clearly separated from the average level. This tendency is also partially present in the case of a moderate spark advance angle $\Delta\alpha = 15°$ (Fig. 2) but note that it is completely absent for $\Delta\alpha = 5°$. However, in the last case, studying more carefully, one can recognize a weak modulation of the Q_i points. The time scale of modulation can be estimated as about 100 engine cycles long.

Examining return maps plotted in Fig. 4a–c one can notice, at the first glance, that they are very similar to each other and also typical for a system without misfires [12,25,31]. Note, there are no specific patterns here as could be expected for deterministic systems. Thus, the first conclusion is that consecutive points are rather weakly correlated or affected by random noise [33].

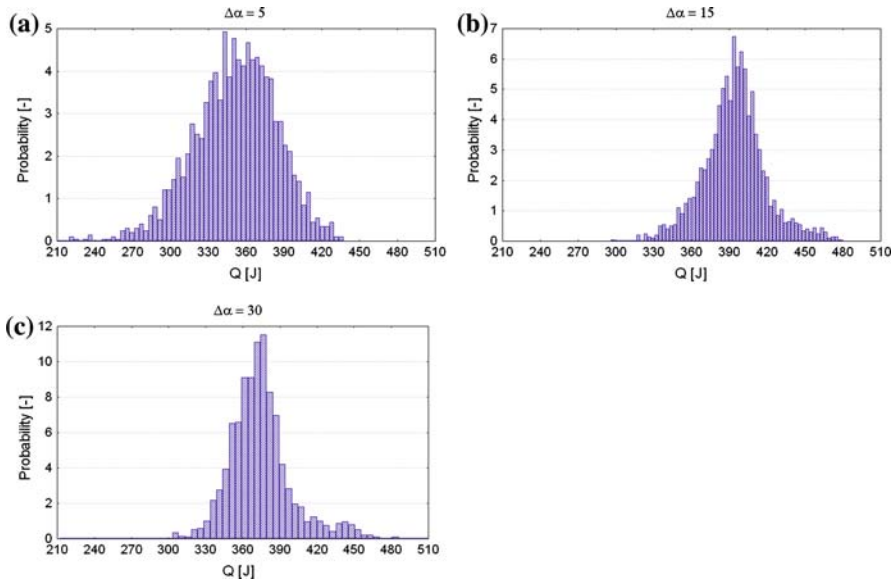

Fig. 3 Histograms of heat release for different spark advance angles: (**a**) $\Delta\alpha = 5°$, (**b**) $\Delta\alpha = 15°$, (**c**) $\Delta\alpha = 30°$

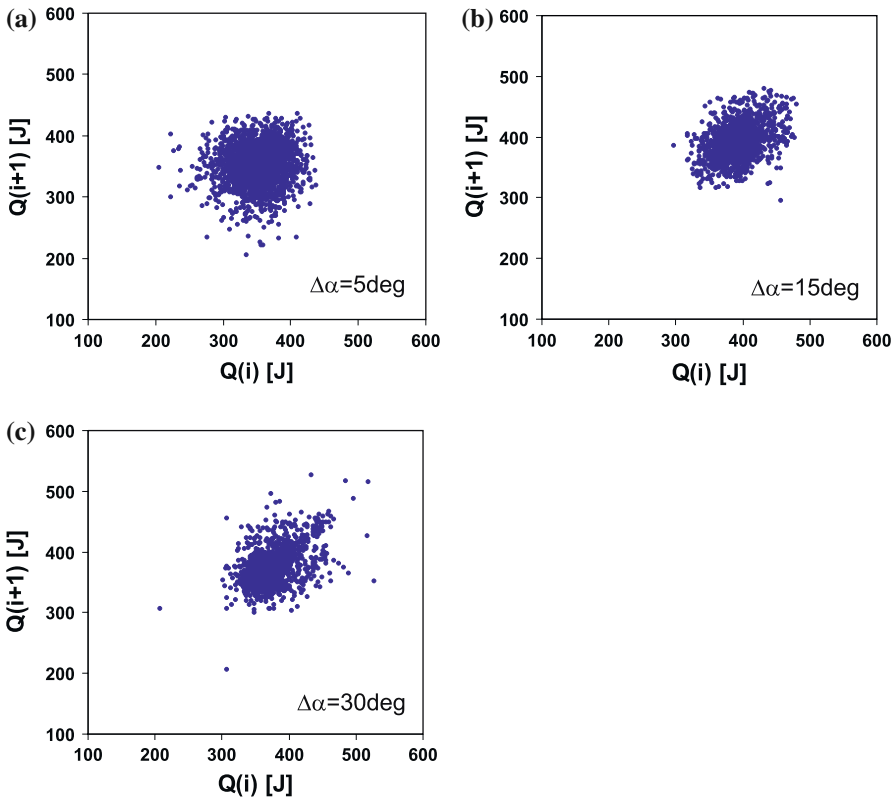

Fig. 4 Return maps of heat release $Q(i+1) = Q_{i+1}$ versus $Q(i) = Q_i$ for different spark advance angles: (**a**) $\Delta\alpha = 5°$, (**b**) $\Delta\alpha = 15°$, (**c**) $\Delta\alpha = 30°$

When the return maps are examined more carefully, some small differences in points distribution are also visible. The second conclusion is that these differences are connected with different ranges of standard deviation σ_Q for each of considered spark advance angles $\Delta\alpha$.

Third, changes in distributions observed in Fig. 3 influence the outer limit points of the distribution in Fig. 4a–c. For instance, the tail on the right hand side of the histogram in Fig. 3c produces additional deviations from the average in the upper and right parts of the return map in Fig. 4c. On the other hand, for the smallest of considered advance angles ($\Delta\alpha = 5°$) the deviations are going in the opposite direction, while the map for the case $\Delta\alpha = 15°$ is the most symmetric, showing the smallest number of deviations. Deviation characteristics observed in return maps are possibly connected with the evidences of a broken time-reversal symmetry of heat release time series noticed by Wagner et al. [12] and Daw et al. [13,22]. However, comparing to their results we do not observe so clear asymmetry in the distribution of points (in the return maps) about the 45° diagonals. Interestingly, the deviation for the smallest spark advance angle $\Delta\alpha = 5°$ (Fig. 4a) indicates that among average cycles there are also cycles with partial combustion while for the largest $\Delta\alpha = 30°$, excluding one singular point (Fig. 4c), we observe rather cycles with very good combustion.

3.2 Intermittent character of heat release changes

Recurrence plots, which were invented by Eckmann et al. [34], were used later for identification of nonlinear systems with various possible behaviors [35,36]. Such plots are constructed from a phase space vectors by spatial proximity analysis of states Q_i. For arbitrary i and j from the interval $[0, N]$, where N is the total number of points in given series, a black dot on the graph is plotted on the graph if the following condition is fulfilled:

$$\left|Q_i - Q_j\right| < \epsilon, \tag{5}$$

plotted on a square matrix whose axes correspond to the i and j indices. Note, ϵ is a small threshold value adjusted for each time series case separately in such a way to get a good contrast in diagram.

In fact using the above qualitative method for deterministic systems it is possible to classify the dynamics of a examined system by its characteristic patterns showing diagonal, vertical, or horizontal structure of lines [37]. The same method applied to an unknown time series is capable of distinguishing chaotic and stochastic behavior. A pattern for a stochastic system is based on uniform distribution of points in the recurrence plot, while a chaotic system possesses structure of lines with finite lengths. On the other hand, in a case of the intermittent motion [38], a vertical stripe structure is expected [26,39,40]. In principle Q_i and Q_j (Eq. 5) should be substituted by corresponding vectors ($\mathbf{Q}_i$ and $\mathbf{Q}_j$) describing the state of the system in the embedding dimension [36,41] defiled by the delayed coordinates. Namely, they are defined [41]

$$\mathbf{Q}_i = \left[Q_i, Q_{i-\delta i}, Q_{i-2\delta i}, \ldots, Q_{i-(m-1)\delta i}\right], \tag{6}$$

where δi is the time delay and m is the embedding dimension. Thus Eq. 5 defining the recurrence plot can be rewritten in the following matrix form $\mathbf{R}^{m,\epsilon}$ with corresponding elements $R_{ij}^{m,\epsilon}$

$$R_{ij}^{m,\epsilon} = \Theta(\epsilon - |\mathbf{Q}_\mathrm{i} - \mathbf{Q}_\mathrm{j}|) \tag{7}$$

having 0 and 1 elements to be translated into the recurrence plot as an empty place and a black dot, respectively. Webber and Zbilut [37] and later Marwan [42] developed the recurrence quantification analysis (RQA) for recurrence plots. First of all the RQA analysis include the recurrence rate RR

$$\mathrm{RR} = \frac{1}{N^2}\sum_{i,j=1}^{N} R_{ij}^{m,\epsilon}, \tag{8}$$

which calculates the black dots in the plot. Furthermore, the RQA can be used to identify vertical or diagonal lines through their maximal lengths $L_{\max}$, $V_{\max}$ for diagonal and vertical lines, respectively. In it frame RQA enables to perform probability $p(l)$ or $p(v)$ distribution analysis of lines according to their length l or v (for diagonal and vertical lines). Practically they are calculated

$$p(x) = \frac{P^\epsilon(x)}{\sum_{x=x_{\min}}^{N} P^\epsilon(x)}, \tag{9}$$

where $x = l$ or v depending on diagonal or vertical structures in the specific recurrence diagram. $P^\epsilon(x)$

denotes unnormalized probability for a given threshold value ϵ. In this way Shannon information entropies (L_{ENTR} and V_{ENTR}) can be defined for diagonal and vertical lines collections

$$L_{\mathrm{ENTR}} = -\sum_{l=l_{\min}}^{N} p(l)\ln p(l), \tag{10}$$

$$V_{\mathrm{ENTR}} = -\sum_{v=v_{\min}}^{N} p(v)\ln p(v). \tag{11}$$

Other properties as determinism DET and laminarity LAM and the trapping time TT are also basing on probabilities $P^{\epsilon}(x)$

$$\mathrm{DET} = \frac{\sum_{l=l_{\min}}^{N} l P^{\epsilon}(l)}{\sum_{i,j=1}^{N} R_{i,j}^{m,\epsilon}}, \tag{12}$$

$$\mathrm{LAM} = \frac{\sum_{v=v_{\min}}^{N} v P^{\epsilon}(v)}{\sum_{v=1}^{N} v P^{\epsilon}(v)}, \tag{13}$$

$$\mathrm{TT} = \frac{\sum_{v=v_{\min}}^{N} v P^{\epsilon}(v)}{\sum_{v=v_{min}}^{N} P^{\epsilon}(v)}, \tag{14}$$

where $l_{\min}$ and $v_{\min}$ denotes minimal values which should be chosen for a specific dynamical system. In our calculations we have assumed $l_{\min} = v_{\min} = 2$.

Determinism DET is the measure of the predictability of the examined time series gives the ratio of recurrent points formed in diagonals to all recurrent points. Note in a periodic system all points would be included in the lines. On the other hand, laminarity LAM is a similar measure which corresponds to points formed in vertical lines. This measure is telling about dynamics behind sampling points changes. For small point-to-point changes the consecutive points form a vertical line. Finally, trapping time TT refers the average length of vertical lines measuring the time scale (in terms of sampling intervals) of these small changes in the examined time history.

For given values of dimension analysis [43] $\Delta\alpha = 5^{\circ}$ ($\delta i = 4$ and $m = 4$) $\Delta\alpha = 15^{\circ}$ ($\delta i = 4$ and $m = 3$) and ($\delta i = 4$ and $m = 4$) time series Q_i and Q_j were represented as vectors $\mathbf{Q}_i$ and $\mathbf{Q}_j$ (Eq. 6).

For all considered cases of $\Delta\alpha = 5^{\circ}$, 15° and 30° plots concerning time series heat release Q_i (Fig. 2) were plotted recurrence plots in Fig. 5a–f. Note recurrence plots in Fig. 5b, d, f correspond to vector representation of heat release time series $\mathbf{Q}_i$ while Fig. 5a, c, e have scalar representation Q_i. Calculations have been done using the code developed by Marwan [44]. For each case (Fig. 5a–f) the threshold value ϵ has be chosen is such away to give the same recurrence rate $\mathrm{RR} = 0.06$.

Interestingly, patterns in a recurrence plot change rapidly as the spark advance angle $\Delta\alpha$ increases. Starting from a relatively uniform distribution of points $\Delta\alpha = 5^{\circ}$ more a structure composed of vertical and horizontal lines are observed for the $\Delta\alpha = 15^{\circ}$ and 30° cases. In particular Fig. 5e, f ($\Delta\alpha = 30^{\circ}$) shows a collection of lines of different lengths. This is clear confirmation of intermittent behavior [39,40]. Note that this supports the conjecture from the previous section about intermittent transition to combustion events of higher efficiency. On the other hand, for $\Delta\alpha = 15^{\circ}$ lines are much thicker, longer and more regular than for $\Delta\alpha = 30^{\circ}$. Referencing the histograms one can observe that some changes in system dynamics are taking place while changing $\Delta\alpha = 15^{\circ}$ into 30° and this fact is resulting in more transparent vertical line structures in Fig. 5e, f.

One can see that some of the features are similar in scalar and vector representations but one has to remember that all invariants of RQA are changing with an embedding space [42,45,46]. In fact the evolution of vertical lines pattern are more transparent for recurrence plots obtained in proper dimensional analysis.

The results of the RQA are summarized in Table 2 and Fig. 6a–c. They unambiguously tell about increasing the vertical structures with increasing advance angle. This applies especially to the increasing tendencies given by points denoted by '2' in the considered Fig. 6a–c.

Note that, in our case, fast combustion gives a higher loading torque, but the combustion is not stable. It is because of worse quality of a combustion mixture (in average), which has to be prepared in a relatively shorter time interval. Such a nonuniform mixture has poor combustion properties and can be only partially burned. The intermittency mechanism may be associated with fluctuating composition of residual gases, and fresh fuel and air given in each new combustion cycle.

4 Summary and conclusions

In the present paper, fluctuations in cyclic heat release time series Q_i have been analyzed. Changing

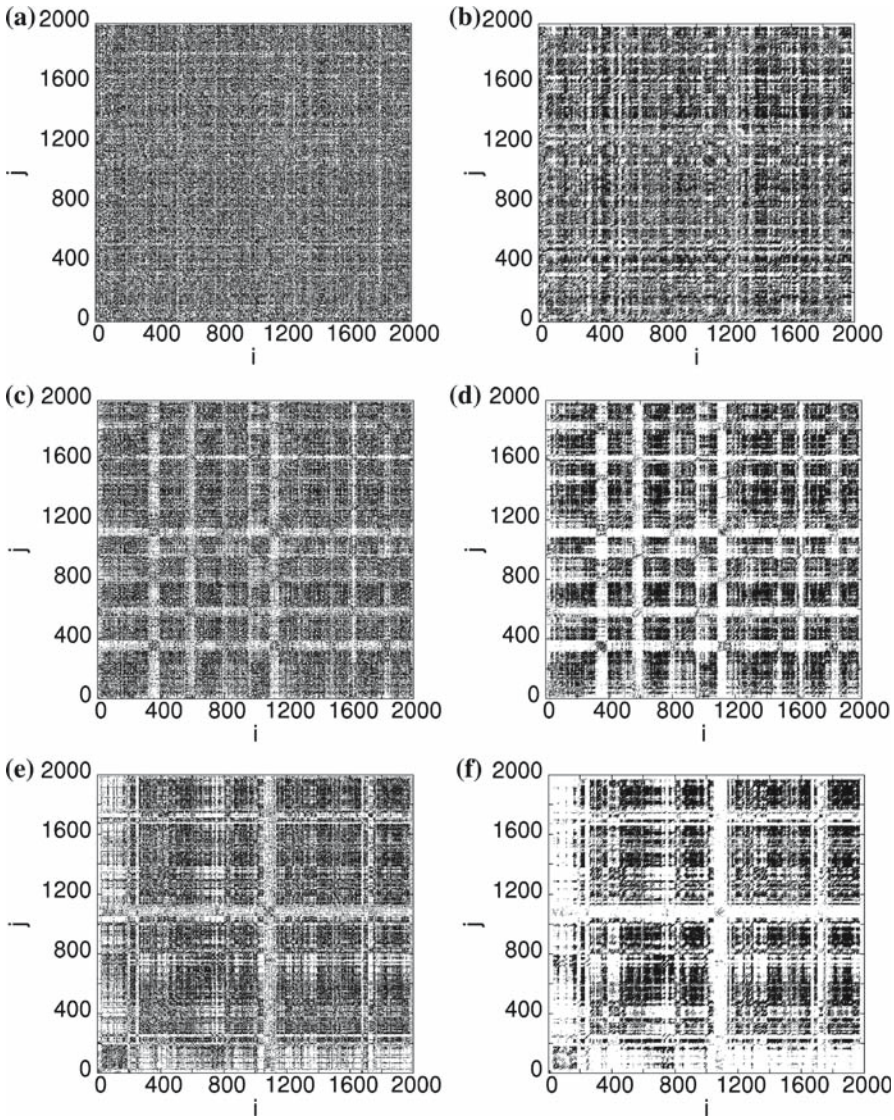

Fig. 5 Recurrence plots for various advance angles $\Delta\alpha$ and different embedding parameters $(m, \delta i)$: (**a**) $\Delta\alpha = 5°$, $(m, \delta i) = (1, 0)$; (**b**) $\Delta\alpha = 5°$, $(m, \delta i) = (4, 4)$; (**c**) $\Delta\alpha = 15°$, $(m, \delta i) = (1, 0)$; (**d**) $\Delta\alpha = 15°$, $(m, \delta i) = (3, 4)$; (**c**) $\Delta\alpha = 30°$, $(m, \delta i) = (1, 0)$; (**d**) $\Delta\alpha = 30°$, $(m, \delta i) = (4, 4)$. In all cases the threshold value ϵ was fitted to keep the recurrence rate RR on the same level (RR = 0.06)

the spark advance angle $\Delta\alpha$ from 5° through 15° to 30°, changes appeared not only in data noise level σ_Q (visible also in Fig. 2) but also in probability distribution, including a characteristic tail for $\Delta\alpha = 30°$ (Fig. 3c). The results were confirmed further by using return maps which showed differences in the distribution of outer limit points. All obtained return maps for Q_i we smeared indicating that the whole system was strongly affected by random noise.

Note that similar results were obtained and analyzed by other researchers working mainly in lean combustion conditions ($\lambda > 1$) where the non-periodic fluctuations seems to be even more transparent [6,12,21,22,47]. For such conditions fuel consumption is smaller but combustion fluctuations increase to higher level including misfires which are getting more probable. The present analysis has been performed for the case of stoichiometric combustion ($\lambda \approx 1$) following works of Kamiński et al. [15].

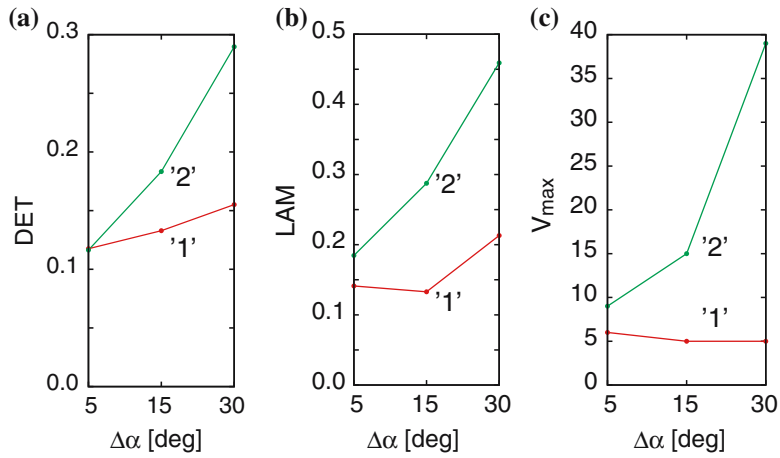

Fig. 6 Recurrence quantification analysis results for heat release time series Q_i: (**a**) DET—determinism, (**b**) LAM—laminarity and (**c**) $V_{\max}$—the maximal length of vertical lines. Line '1' corresponds to scalar signal analysis of heat release (Q_i) while '2' for ($\mathbf{Q}_i$) defined in the embedding space. The recurrence rate RR = 0.06 in all cases

Table 2 Summary of recurrence quantification analysis (RQA) of heat release Q for different advance angle $\Delta\alpha$

$\Delta\alpha$	m	δi	DET	LAM	$L_{\max}$	L_{ENTR}	$V_{\max}$	V_{ENTR}	TT
5°	1	0	0.1175	0.1412	5	0.2349	6	0.2410	2.065
15°	1	0	0.1329	0.1329	5	0.2755	5	0.3521	2.107
30°	1	0	0.1551	0.2131	5	0.3348	5	0.4853	2.171
5°	4	4	0.1164	0.1846	11	0.2304	9	0.3874	2.123
15°	3	4	0.1833	0.2875	9	0.4038	15	0.6176	2.251
30°	4	4	0.2897	0.4591	27	0.6389	39	1.0250	2.662

Note, embedding parameters $(m, \delta i) = (1, 0)$ corresponds to scalar signal analysis (scalar time series of heal release Q_i), while $(m, \delta i) = (4, 4)$ or $(3, 4)$ are for vector signal analysis ($\mathbf{Q}_i$ [43]). In all cases the recurrence rate $RR = 0.06$

Its is worth noting that different spark advance angles $\Delta\alpha$ correspond to different regions in the maximum pressure versus angle diagram ($p_{\max}, \alpha_{\mathrm{pmax}}$). Such a diagram covering all examined angles $\Delta\alpha$ is plotted in Fig. 7. It is interesting that $\Delta\alpha$ directly affects the time scale of combustion process [28]. Its larger values $\Delta\alpha = 15°$ and 30° speed this phenomenon. In fact $\Delta\alpha = 30°$ seems to be already too fast, causing combustion in the spark plug neighborhood instead of the whole cylinder. In contrast the smallest spark advance angle ($\Delta\alpha = 5°$) can be associated with slow combustion. In that case, however, the fuel mixture is not uniform. In some areas it is rich and in others is lean, which favor partial combustion. Paradoxically, combustion conditions associated with the largest $\Delta\alpha = 30°$ lead to a similar result. Now combustion seems to be too fast to propagate its flame front to the whole volume of the cylinder causing non-effective combustion limited to area around an spark plug. Evidently the case with a moderate spark advance angle ($\Delta\alpha = 15°$) is a reasonable compromise between two others in the present working conditions of the engine. Note that this confirms the authors' previous findings about optimal combustion conditions in [15] where the noise level in heat release time series is evaluated. However, the suggested optimal timing $\Delta\alpha = 15$ degrees obtained from heat release oscillations minimization not necessarily the timing that would be selected for maximum brake torque, which is usually applied in spark ignition engines.

Acknowledgements The authors would like to acknowledge a partial support from the Polish State Committee of Scientific Research. GL is grateful to prof. J. Kurths for hospitality during his visit to Potsdam University and for illuminating discussions.

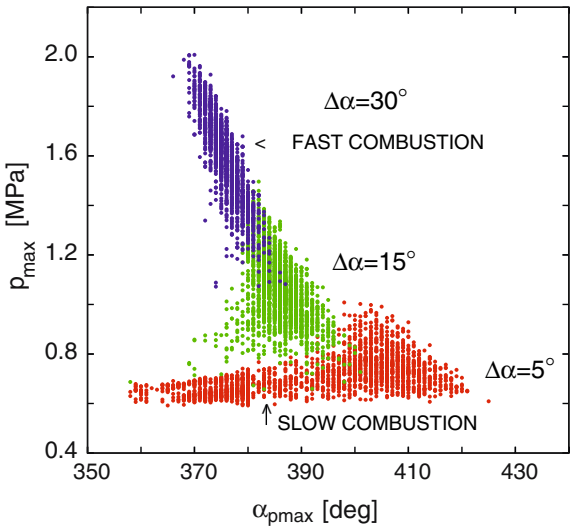

Fig. 7 Cyclic maximum pressure versus its angle diagram $(p_{\max}, \alpha_{\mathrm{pmax}})$ for different spark advance angles $\Delta\alpha = 5°$, $\Delta\alpha = 15°$, $\Delta\alpha = 30°$

The authors are also grateful to unknown reviewers for their remarks.

References

1. Clerk D (1886) The gas engine. Longmans Green & Co., London
2. Patterson DJ (1966) Cylinder pressure variations, a fundamental combustion problem. SAE paper No. 660129.
3. Hubbard M, Dobson PD, Powell JD (1976) Closed loop control of spark advance using a cylinder pressure sensor. J Dyn Syst Measure Contro 98:414–420
4. Matekunas FA (1986) Engine combustion control with ignition timing by pressure ratio management. US Pat., A 4622939 Nov. 18
5. Sawamoto K, Kawamura Y, Kita T, Matsushita K (1987) Individual cylinder knock control by detecting cylinder pressure. SAE paper No. 871911
6. Wagner RM, Daw CS, Thomas JF (1993) Controlling chaos in spark-ignition engines. In: Proceedings of the central and Eastern states joint technical meeting of the combustion institute, New Orleans, March 15–17
7. Eriksson L, Nilsen L, Glavenius M (1997) Development of control algorithm stabilizing torque for optimal position of pressure peak. SAE Trans J Engines 106:1216–1223
8. Müller R, Hemberger H-H, Baier KH (2001) Engine control using neural networks: a new method in Engine Management systems. Meccanica 32:423–430
9. Kantor JC (1984) A dynamical instability of spark-ignited engines. Science 224:1233–1235
10. Heywood JB (1988) Internal combustion engine fundamentals. McGraw-Hill, New York
11. Hu Z (1996) Nonlinear instabilities of combustion processes and cycle-to-cycle variations in spark-ignition engines. SAE paper No. 961197
12. Wagner RM, Drallmeier JA, Daw CS (2001) Characterization of lean combustion instability in pre-mixed charge spark ignition engines. Int J Engine Res 1:301–320
13. Daw CS, Finney CEA, Tracy ER (2003) A review of symbolic analysis of experimental data. Rev Scien Instr 74:915–930
14. Wendeker M, Czarnigowski J, Litak G, Szabelski K (2003) Chaotic combustion in spark ignition engines. Chaos, Solitons Fractals 18:803–806
15. Kamiński T, Wendeker M, Urbanowicz K, Litak G (2004) Combustion Process in a Spark Ignition Engine: Dynamics and Noise Level Estimation. Chaos 14:461–466
16. Winsor RE, Patterson DJ (1973) Mixture turbulence – a key to cyclic combustion variation. SAE paper No. 730086
17. Daily JW (1988) Cycle-to-cycle variations: a chaotic process?. Combust Sci Technol 57:149–162
18. Foakes AP, Pollard DG (1993) Investigation of a chaotic mechanism for cycle-to-cycle variations. Combust Sci Technol 90:281–287
19. Chew L, Hoekstra R, Nayfeh JF, Navedo J (1994) Chaos analysis of in-cylinder pressure measurements. SAE Paper No. 942486
20. Letellier C, Meunier-Guttin-Cluzel S, Gouesbet G, Neveu F, Duverger T, Cousyn B (1997) Use of the nonlinear dynamical system theory to study cycle-to-cycle variations from spark-ignition engine pressure data. SAE Paper No. 971640
21. Daw CS, Finney CEA, Green Jr, JB, Kennel MB, Thomas JF, Connolly FT (1996) A simple model for cyclic variations in a spark-ignition engine. SAE paper No. 962086
22. Daw CS, Kennel MB, Finney CEA, Connolly FT (1998) Observing and modelling dynamics in an internal combustion engine. Phys Rev E 57:2811–2819
23. Rocha-Martinez JA, Navarrete-Gonzalez TD, Pavia-Miller CG, Paez-Hernandez R, Angulo-Brown F (2002) Otto and diesel engine models with cyclic variability. Revista Mexicana de Fisica 48:228–234
24. Litak G, Taccani R, Radu R, Urbanowicz K, Wendeker M, Hołyst JA, Giadrossi A (2005) Estimation of the noise level using coarse-grained entropy of experimental time series of internal pressure in a combustion engine. Chaos, Solitons Fractals 23:1695–1701
25. Green Jr JB, Daw CS, Armfield JS, Finney CEA, Wagner RM, Drallmeier JA, Kennel MB, Durbetaki P (1999) Time irreversibility and comparison of cyclic-variability models. SAE Paper No. 1999-01-0221
26. Wendeker M, Litak G, Czarnigowski J, Szabelski K (2004) Nonperiodic oscillations in a spark ignition engine. Int J Bif Chaos 14:1801–1806
27. Sen AK, Litak G, Taccani R, Radu R (2007) Wavelet analysis of cycle-to-cycle pressure variations in an internal combustion engine. Chaos, Solitons Fractals (in press), doi:10.1016/j.chaos.2007.01.047
28. Ozdor N, Dulger M, Sher E (1994) Cyclic variability in spark ignition engines: a literature survey. SAE paper No. 940987

29. Radu R, Taccani R (2003) Experimental setup for the cyclic variability analysis on a spark ignition engine. SAE NA No. paper 2003-01-19
30. Litak G, Wendeker M, Krupa M, Czarnigowski J (2005) A numerical study of a simple stochastic/deterministic model of cycle-to-cycle combustion fluctuations in spark ignition engines. J Vibration Control 11:371–379
31. Piernikarski D, Hunicz J (2000) Investigation of misfire nature using optical combustion sensor in a SI automotive engine. SAE paper No. 2000-02-0549
32. Radons G, Neugebauer R (eds) (2004) Nonlinear dynamic effects of production systems. Wiley-VCH, Weinheim
33. Sprott JC (2003) Chaos and time series analysis. Oxford University Press, New York
34. Eckmann J-P, Kamphorst SO, Ruelle D (1987) Recurrence plots of dynamical systems. Europhys Lett 5:973–977
35. Casdagli MC (1997) Recurrence plots revisited. Physica D 108:12–44
36. Kantz H, Schreiber T (1997) Nonlinear time series analysis. Cambridge University Press, Cambridge
37. Webber CLJr , Zbilut JP (1994) Dynamical assessment of physiological systems and states using recurrence plot strategies. J Appel Physiol 76:965–973
38. Chatterjee S, Malik AK (1996) Three kinds of intermittency in a nonlinear system. Phys Rev E 53:4362–4367
39. Marwan N, Wessel N, Meyerfeldt U, Schirdewan A, Kurths J (2002) Recurrence-plot-based measures of complexity and their application to heart-rate-variability data. Phys Rev E 66:026702
40. Marwan N, Meinke A (2004) Extended recurrence plot analysis and its application to EPR data. Int J Bif Chaos 14:761–771
41. Takens F (1981) Detecting strange attractors in turbulence. Lecture Notes in Mathematics, vol 898. Springer, Heidelberg, pp 366–381
42. Marwan N (2003) Encounters with Neighbours: Current Development of Concepts Based on Recurrence Plots and their Applications PhD Thesis. Universität Potsdam, Potsdam
43. Litak G, Kamiński T, Rusinek R, Czarnigowski J, Wendeker M (2007) Patterns in the combustion process in a spark ignition engine. Chaos, Solitons Fractals (in press), doi:10.1016/j chaos.2006.05.053
44. Marwan N (2006) Recurrence plots code. http:// www.agnld.uni- potsdam.de/∼marwan/6.download/rp.php
45. Thiel M, Romano MC, Read PL, Kurths J (2004) Estimation of dynamical invariants without embedding by recurrence plots. Chaos 14:234–243
46. Balibrea F, Caballero MV, Molera L (2007) Recurrence quantification analysis in Liu's attractor. Chaos, Solitons Fractals (in press), doi:10.1016/j choas.2006.06.107
47. Wagner RM, Drallmeier JA, Daw CS (1998) Prior-cycle effects in lean spark ignition combustion: fuel/air charge considerations. SAE Paper No. 981047